Experimental Eye Research 194 (2020) 108004

Contents lists available at ScienceDirect

Experimental Eye Research

journal homepage: www.elsevier.com/locate/yexer

VEGF receptor 2 inhibitor nintedanib completely reverts VEGF-A_{165}-induced disturbances of barriers formed by retinal endothelial cells or long-term cultivated ARPE-19 cells

Heidrun L. Deissler[a,*], Jan-Niklas Stutzer[b,c], Gerhard K. Lang[a], Salvatore Grisanti[b], Gabriele E. Lang[a], Mahdy Ranjbar[b,c]

[a] Department of Ophthalmology, University of Ulm Hospital, Ulm, Germany
[b] Department of Ophthalmology, University of Luebeck, Luebeck, Germany
[c] Laboratory for Angiogenesis and Ocular Cell Transplantation, University of Luebeck, Luebeck, Germany

ARTICLE INFO

Keywords:
Retinal endothelial cells
Retinal pigment epithelial cells
VEGF-A
VEGF receptor
Blood-retina barrier
Permeability
Tight junctions
VEGF-A-induced signal transduction

ABSTRACT

Various severe ocular diseases are associated with an elevated intravitreal expression of VEGF-A which increases the permeability of retinal endothelial cells (REC) or retinal pigment epithelial (RPE) cells *in vivo* and *in vitro*. Inhibition of VEGF receptor 2 (VEGFR2) is sufficient to completely prevent VEGF-A_{165}-induced dysfunctions of barriers formed by long-term cultivated, immortal human ARPE-19 cells or immortalized bovine retinal endothelial cells (iBREC). Extended exposure to VEGF-A could result in additional activation of other growth factor receptors, potentially promoting synergistic effects of corresponding factors on various cellular processes including angiogenesis. Based on these observations, we investigated whether blocking of VEGFR2 is also sufficient to revert VEGF-A-induced changes of the barriers consisting of iBREC (i.e. inner blood-retina barrier) or ARPE-19 cells (i.e. outer blood-retina barrier) *in vitro*. Alterations of confluent monolayers' properties induced by treatment with VEGF-A_{165} for one day followed by addition of small molecule inhibitors of the VEGFR2 were determined by continuous cell index (CI) measurements using the microelectronic biosensor system for cell-based assays xCELLigence. VEGF-A_{165} induced a long-lasting drop of the otherwise high CI of iBREC accompanied by reduced expression of the tight junction (TJ) protein claudin-1 and subtle changes of the plasma membrane localizations of TJ-protein claudin-5 and of vascular endothelial cadherin. Blocking mainly VEGFR2 with 10 nM nintedanib, 10 nM tivozanib or 500 nM ZM323881 efficiently reverted these changes within one day; higher concentrations of nintedanib or additional inhibition of neuropilin-1 were not superior. Interestingly, the CI of short-term cultivated, confluent ARPE-19 cells slightly increased in the presence of VEGF-A_{165}, but was not changed by nintedanib. In contrast, VEGF-A_{165} markedly reduced the transepithelial electrical resistance of ARPE-19 cells cultivated on porous membrane inserts for three weeks, which was also accompanied by a significant loss of the then strongly plasma membrane-expressed TJ-protein ZO-1. These alterations were completely reverted within one day by 10 nM nintedanib of which higher concentrations were not superior. None of the inhibitors tested diminished the strong barrier properties of iBREC or long-term cultivated ARPE-19 cells. Taken together, inhibition of VEGFR2 efficiently reverts VEGF-A_{165}-induced barrier disturbances of both cell types forming and regulating the inner and outer blood-retina barrier. As synergistic actions of growth factors seem to play only a minor role in inducing a barrier dysfunction, specific inhibition of VEGFR2 could be an interesting option to treat VEGF-A-induced macular edema without obvious effects on vitality and functions of REC and RPE cells.

1. Introduction

Vascular endothelial growth factor-A (VEGF-A) is crucially involved in the pathogeneses of various ocular diseases of high socio-economic relevance: Diabetic retinopathy, diabetic macular edema, retinal vein occlusion or age-related macular degeneration (Ambati et al., 2003; Ozaki et al., 1999; Qaum et al., 2001). Levels of VEGF-A in the vitreous fluid were found to be elevated, resulting in the break-down of the

* Corresponding author. Department of Ophthalmology, University of Ulm, Prittwitzstrasse 43, 89075, Ulm, Germany.
E-mail address: heidrun.deissler@uniklinik-ulm.de (H.L. Deissler).

https://doi.org/10.1016/j.exer.2020.108004
Received 1 October 2019; Received in revised form 11 March 2020; Accepted 11 March 2020
Available online 14 March 2020

Abbreviations

A7R	NH_2-ATWLPPR-COOH
AJ	adherens junction
BRB	blood-retina barrier
CI	cell index
DMSO	dimethyl sulfoxide;
EC	endothelial cells
ECGM	endothelial cell growth medium
FBS	fetal bovine serum
FGF/FGFR	fibroblast growth factor/fibroblast growth factor receptor
FM	full medium
hEGF	human epidermal growth factor
HRP	horseradish peroxidase
(i)BREC	(immortalized) bovine retinal microvascular endothelial cells
IF	immunofluorescence
MTT	3-(4,5-dimethylthiazol-2-yl)-2,5-diphenyltetrazolium bromide;
NRP-1	neuropilin 1
PBS	phosphate-buffered saline,
PDGF/PDGFR	platelet-derived growth factor/platelet-derived growth factor receptor
P*l*GF	placental growth factor
REC	retinal microvascular endothelial cells
RPE	retinal pigment epithelial
SRM-REC	serum-reduced culture medium for retinal endothelial cells
SRM-RPE	serum-reduced culture medium for retinal pigment epithelial cells
TEER	transepithelial electrical resistance
TJ	tight junction
VEcadherin	vascular endothelial cadherin
VEGF-A/VEGFR	vascular endothelial growth factor-A/vascular endothelial growth factor receptor
WB	Western blot
ZO-1	zonula occludens-1

blood-retina barrier (BRB) and in neovascularization of retinal or choroidal vessels (Aiello et al., 1994; Campochiaro 2000, 2013; Kliffen et al., 1997; Qaum et al., 2001). VEGF-A not only causes elevated permeability of microvascular retinal endothelial cells (REC) of the inner blood-retina barrier *in vivo* but also destabilizes the barrier consisting of primary or immortalized REC of human or bovine origin *in vitro*. This is associated with changes in the compositions of tight junctions (TJs) or adherens junctions (AJs) and altered transcellular transport (Antonetti et al., 1999; Deissler et al., 2008, 2011; Suarez et al., 2014). On the molecular level, the most significant change induced by extended exposure of immortalized bovine REC (iBREC) to VEGF-A_{165} is the reduced expression of the TJ-protein claudin-1 and its delocalization from the plasma membrane. These effects become evident about 6 h after addition of the growth factor which correlates with decreased transendothelial electrical resistance or cell index (CI) as measures of cell monolayer permeability (Deissler et al., 2011, 2017). Subtle alterations of the plasma membrane localizations of claudin-5 and the AJ-protein vascular endothelial cadherin (VEcadherin) were also observed after addition of VEGF-A_{165} to primary or immortalized BREC, or human REC (Deissler et al., 2011, 2013a, 2017; Dejana et al., 2009; Jeong et al., 2016; Kim and Suh, 2017).

The outer blood-retina barrier, mainly determined by the properties of a monolayer of retinal pigment epithelium (RPE) cells, regulates the passage of molecules between the retina and the choriocapillaris (Cunha-Vaz, 2017; Strauss, 2005). Furthermore, RPE cells produce various cytokines such as VEGF-A, platelet derived growth factor (PDGF), and fibroblast growth factor (FGF) (Ford et al., 2011; McLaren and Inana, 1997; Nagineni et al., 2005). Exposure of primary and immortal, long-term cultivated RPE cells to exogenously added VEGF-A_{165} *in vitro* results in a considerably drop of their transepithelial electrical resistance (TEER) determined as a measure of permeability (Ablonczy and Crosson, 2007; Ablonczy et al., 2011; Miyamoto et al., 2007). Prolonged cultivation of immortal human ARPE-19 cells is associated with their polarization including polarized protein expression and polarized secretion of growth factors (Dunn et al., 1996, 1998; Kannan et al., 2006; Geisen et al., 2006; Miyamoto et al., 2007; Ablonczy et al., 2011; Ford and D'Amore, 2012). The cells of the RPE exhibit TJs, AJs, and gap junctions and of these, TJs have been shown to be most important with regard to regulation of RPE permeability: After exposure to VEGF-A_{165}, disruption of the otherwise continuous dispersion of the TJ-protein zonula occludens-1 (ZO-1) over the plasma membrane was observed (Ablonczy and Crosson, 2007; Ablonczy et al., 2011).

VEGF-A_{165} is linked to intracellular signal transduction pathways through binding to the VEGF receptors VEGFR1, VEGFR2 or neuropilin 1 (NRP-1), which are all expressed by REC and RPE cells (Ferrara, 2004; Deissler et al., 2011; Ablonczy et al., 2009; Bai et al., 2013). Inhibition of only VEGFR2 with small molecule inhibitors completely prevented barrier dysfunction of long-term cultivated, immortal human ARPE-19 and primary porcine RPE cells observed shortly after addition of VEGF-A_{165} (Ablonczy and Crosson, 2007). After similar treatment of iBREC, the preventive effect of VEGFR2 inhibitors even lasted several days (Deissler et al., 2017). Additional blocking of the VEGFR1 was not more efficient, indicating that VEGF-A-induced permeability of layers of both cell types is likely a consequence of VEGFR2-mediated signaling (Ablonczy and Crosson, 2007; Deissler et al., 2017). Extended exposure of cells to VEGF-A might however result in the activation of other growth factor receptors or intracellular protein kinases, as cross talk between proteins involved in various growth factor-induced signaling processes can play a role in angiogenesis (Castellon et al., 2002; Li et al., 2016; Stahl et al., 2009). Therefore, we studied whether inhibition of only VEGFR2 is indeed sufficient to revert VEGF-A-induced barrier disturbances of iBREC or ARPE-19 cells, which are well-accepted *in vitro* models resembling the inner and outer blood-retina barrier, respectively.

2. Materials and Methods

2.1. Reagents and antibodies

Recombinant human *Sf*21-expressed VEGF-A_{165} (293VE) was purchased from bio-techne (Wiesbaden, Germany). Inhibitors - listed in Table 1 - were bought from Selleckchem (Selleckchem via Absource GmbH, Munich, Germany) except for peptide NH_2-ATWLPPR-COOH (A7R) from Eurogentec (Seraing, Belgium). These substances were dissolved in dimethyl sulfoxide (DMSO; Sigma-Aldrich, Steinheim, Germany) to result in final solvent concentrations below 0.05% in the culture medium which did not affect cell morphology or behavior. Antibodies used in this study are listed in Table 2.

2.2. Cultivation and treatment of iBREC with VEGF-A_{165} and/or inhibitors

Generation and characterization of telomerase-immortalized microvascular endothelial cells from bovine retina (iBREC) have been described in detail elsewhere (Deissler et al., 2005). Cells were used between passages 25 and 55 counting from the stage of primary culture, for which we confirmed stable expression of investigated proteins and marker proteins typical for EC, e.g. von Willebrand factor, VEcadherin, claudin-1, and claudin-5 (Deissler et al., 2005, 2008, 2011, 2013a). As

Table 1
Characteristics of inhibitors used.

Inhibitor	Targeted protein	IC_{50}	Final concentrations	References
Nintedanib	VEGFR1	34 nM	10 nM and 100 nM	Hilberg et al. (2008)
(BIBF1120)	VEGFR2	21 nM		
	VEGFR3	13 nM		
	FGFR1	69 nM		
	FGFR2	37 nM		
	FGFR3	108 nM		
	PDGFRα	59 nM		
	PDGFRβ	65 nM		
Tivozanib	VEGFR1	30 nM	10 nM	Nakamura et al. (2006)
(KRN951, AV-951)	VEGFR2	6.5 nM		
	VEGFR3	15 nM		
	PDGFRα	40 nM		
	PDGFRβ	49 nM		
ZM323881	VEGFR1	> 50 μM	500 nM	Whittles et al. (2002)
	VEGFR2	< 2 nM		
NH_2-ATWLPPR-COOH (A7R)	NRP-1	19 μM	50 μM	Tirand et al. (2006)

additional confirmation of iBREC authenticity and viability, we routinely recorded their characteristic proliferation profile by electric cell-substrate impedance measurements (see 2.8) (Deissler et al., 2017). Cultures of iBREC were free of α-smooth muscle actin expressing cells.

iBREC were cultivated in Endothelial Cell Growth Medium MV (ECGM; Promocell, Heidelberg, Germany) containing 1 g/l glucose, 0.4% Endothelial Cell Growth Supplement/H, 90 μg/ml heparin, 10 ng/ml human epidermal growth factor (hEGF), 100 nM 11β-hydroxycortisone and 5% fetal bovine serum (FBS) on fibronectin-coated (50 μg/ml; BD Biosciences, Corning, Amsterdam, The Netherlands) surfaces as previously described (Deissler et al., 2005, 2008, 2011, 2013a). Prior to experiments with confluent iBREC, formed after cultivation in ECGM for three days, the culture medium was replaced with serum-reduced culture medium (SRM-REC; same as ECGM but without hEGF and containing 0.25% FBS and 1 μg/ml fibronectin) for 24 h before the cells were exposed to VEGF-A_{165} (50 ng/ml final concentration). After 24–26 h, inhibitors (for final concentrations, see Table 1) were added to the cells, which were harvested for preparation and analyses of protein extracts 24 h or 48 h later. Due to its limited stability under conditions of cell cultivation, ZM323881 was used at concentration of 500 nM in all experiments (Deissler et al., 2017). To investigate whether nintedanib or the peptide A7R prevented VEGF-A_{165}-induced barrier dysfunction of iBREC monolayers, confluent cells were cultivated in SRM-REC as described above. Then the inhibitor to be investigated was added for 2 h, followed by incubation with 50 ng/ml VEGF-A_{165} for one day. Control cells were processed identically in culture medium only lacking the effector(s) under investigation. To avoid cells' potential responses to pH or temperature fluctuations, fresh culture medium was always pre-equilibrated.

2.3. Cultivation and treatment of ARPE-19 cells with VEGF-A_{165} and/or inhibitors

Immortal human RPE cells (ARPE-19, ATCC, Manassas, Virginia, USA) were cultivated in DMEM/F12 supplemented with 10% FBS and 1% penicillin/streptomycin (FM, full medium), and passages 22 through 28 were used for experiments. As previously reported, cell authenticity was confirmed by short tandem repeat DNA phenotyping (Ranjbar et al., 2016a, 2016b).

Membrane inserts (polyethylene terephthalate, pore size 0.4 μm, Ø 8 mm, Greiner Bio-One GmbH, Frickenhausen, Germany) were coated with laminin (Merck Millipore, Darmstadt, Germany). On these, 5×10^4 cells were seeded and maintained in DMEM/F12 supplemented with only 1% FBS and 1% penicillin/streptomycin (SRM-RPE) for 3 weeks as described previously (Ablonczy and Crosson, 2007; Ablonczy et al., 2011; Ford and D'Amore, 2012; Ranjbar et al., 2016a, 2016b). Culture medium was renewed twice a week and the barrier function of the cells was evaluated by repeated TEER measurements with a Millicell ERS-2 Voltmeter (Merck Millipore) (Fig. 6A). TEERs [Ωcm^2] of an individual cell monolayer at specific time points were calculated as the average of three independent measurements, corrected for background resistance of the blank membrane with culture medium. After a stable TEER (≥ 40 Ωcm^2) was reached and strong expression of ZO-1 was confirmed (Fig. 6B), confluent monolayers of ARPE-19 cells were exposed at their apical side to VEGF-A_{165} (50 ng/ml final concentration) for 24 h. The culture medium in the upper chamber close to the apical side of the cells was replaced by SRM-RPE containing 10 nM or 100 nM nintedanib, respectively. After additional incubation for 24 h, the supernatant was removed from the apical chamber for determination of secreted VEGF-A by ELISA (see 2.6), and cells were processed for immunofluorescence staining (see 2.7). During all experiments, TEER of the cells was measured regularly. Control cells underwent the same experimental procedures in culture medium only lacking the effector(s) under investigation.

2.4. Cell viability assay

ARPE-19 cells (~10^4 per well of a 96-well plate) were allowed to adhere over 24 h in FM before they were exposed to different concentrations of nintedanib (10 nM - 50 μM) or VEGF-A_{165} (5 ng/ml – 100 ng/ml) diluted in SRM-RPE for 24 h. Then 3-(4,5-dimethylthiazol-2-yl)-2,5-diphenyltetrazolium bromide (MTT; final concentration:

Table 2
Primary and secondary antibodies used.

Target	Host and Type	Source	Working Concentrations
actin	mouse, monoclonal	clone AC-40, abcam (Cambridge, UK), ab11003	WB: 500 ng/ml
claudin-1	rabbit, polyclonal	JAY.8, Thermo Fisher Scientific (Langenselbold, Germany), 51-9000	WB: 1 μg/ml
claudin-1	rabbit, polyclonal	Aviva Systems Biology (Biozol, Eching, Germany), ARP33623_P50	IF: 4 μg/ml
claudin-5	rabbit, polyclonal	Z43.JK Thermo Fisher Scientific, 34-1600	WB: 100 ng/ml, IF: 2.5 μg/ml
VEcadherin	rabbit, polyclonal	Cell Signaling Technology B.V. (Frankfurt, Germany), 2158S	WB: 1:1000, IF: 1:100
ZO-1	rabbit, polyclonal	Merck Millipore (Darmstadt, Germany), AB2272	IF: 1:100
whole IgG, rabbit	goat, polyclonal, coupled to HRP	Biorad (Munich, Germany), 170-5046	WB: 1:30000
whole IgG, mouse	goat, polyclonal, coupled to HRP	Biorad, 170-5047	WB: 1:30000
IgG, H + L chains, rabbit	goat, F(ab')$_2$ fragment, coupled to AlexaFluor595	Thermo Fisher Scientific, A11072	IF: 1:500
IgG, H + L chains, rabbit	goat, polyclonal, coupled to DyLight550	Thermo Fisher Scientific, 84541	IF: 1:200

0.5 mg/ml) was added to the culture medium and cells were incubated for 3 h at 37 °C. The formed formazan was solubilized in 100 µl DMSO per well and quantified by photometry based on its light absorption at 570 nm (SpectraMax i3x, Molecular Devices GmbH, Biberach an der Riss, Germany). Alternatively, ARPE-19 cells (~10^4) cultivated for 21 days on laminin-coated membrane inserts as described above (see 2.3) were exposed to different concentrations of nintedanib and VEGF-A_{165}, followed by incubation with MTT.

2.5. Preparation of protein extracts and Western blot analyses

Whole cell extracts from fresh or frozen iBREC pellets were prepared as previously described (Deissler et al., 2011). Alternatively, 2 × 10^6 iBREC were suspended in 300 µl ice-cold lysis buffer 17 (bio-techne) supplemented with 5 µg/ml aprotinin, 10 µg/ml pepstatin, 10 µg/ml leupeptin (all from Roche Diagnostics, Mannheim, Germany) and phosphatase inhibitor cocktail 2 (1:200; Sigma Aldrich), and incubated on ice for 30 min under gentle agitation. After centrifugation (21100 × *g* for 20 min at 4 °C), the supernatant was stored at −80 °C.

Proteins of interest in whole cell lysates from ~3 × 10^5 iBREC were analyzed by Western blotting and chemiluminescence signals were visualized by direct scanning with the imaging system Fusion Pulse TS (Vilbert Lourmat, VWR), resulting in images with bright bands on dark background (Deissler et al., 2017). For signal quantification, peak volumes of the corresponding bands (e.g. specific for claudin-1, claudin-5, or VEcadherin) were determined with Evolution Capt software (Vilbert Lourmat) and standardized in relation to those of actin. To compare independent experiments, values were normalized in relation to those obtained from similar processing of control cells.

2.6. Measuring extracellular VEGF-A

ARPE-19 cells cultivated on membrane inserts were subsequently exposed at their apical side to VEGF-A_{165} and nintedanib as described above (see 2.3) and amounts of VEGF-A present in the supernatant taken from the upper chamber was determined by ELISA (human VEGF Quantikine ELISA Kit, bio-techne) according to the manufacturer's protocol. Signals at 450 nm with the reference wavelength set at 540 nm were determined with a multimode plate reader (SpectraMax M4, Molecular Devices).

2.7. Immunofluorescence staining

Immunofluorescence staining of confluent iBREC to detect and localize proteins of interest (i.e claudin-1, claudin-5 or VEcadherin) was performed as described in detail elsewhere (Deissler et al., 2017).

Localization of the TJ-protein ZO-1 in ARPE-19 cells was determined by immunofluorescence staining of cells cultivated on membrane inserts as described above (see 2.3.). Cells were washed with PBS and fixated in 4% paraformaldehyde, before they were permeabilized and unspecific binding sites blocked by treatment with 0.1% Triton-X 100/5% goat serum in PBS for 2 h at room temperature, followed by incubation with a rabbit anti-human ZO-1 antibody overnight at 4 °C. After washing with PBS, cells were incubated with a DyLight550-conjugated goat-anti-rabbit IgG antibody for 1 h, before 100 µl of 1 µg/ml 4',6-diamidino-2-phenylindole (Thermo Fisher Scientific) were added for 10 min at room temperature. Membranes were washed again with PBS, and cut out along their periphery with a trepan, and mounted between glass slides and cover slips in Mowiol mounting medium (Sigma Aldrich). Fluorescence images (200 × 300 μm^2) were taken with an inverse fluorescence microscope (Leica DMI6000 B, Leica Microsystems, Wetzlar, Germany). Three images of each membrane were used for semi-quantitative determination of the number of DyLight550 (ZO-1)-positive particles with ImageJ software (NIH, Bethesda, USA).

2.8. Cell index measurement

Barrier stability was monitored by continuous electric cell-substrate impedance measurements using the microelectronic biosensor systems for cell-based assays xCELLigence RTCA DP (→ iBREC; Acea, OLS, Bremen, Germany) or xCELLigence RTCA SP (→ ARPE-19 cells; Acea). Impedance was measured between gold electrodes in individual wells of an E-Plate and calculated as the unit-free parameter cell index CI = $(Z_i\text{-}Z_0)/15\ \Omega$ (RTCA Software 2.0, Acea). In this formula, Z_i is the impedance measured at an individual time point and Z_0 the impedance read at the start of the experiment (Sun et al., 2012).

iBREC (~10^4 cells in ECGM) were seeded per fibronectin-coated well of an E-Plate 16 PET (Acea) and cultivated until a confluent monolayer was reached (three to four days later; CI ~ 18), before the culture medium was replaced by 200 µl SRM-REC (Deissler et al., 2017). After incubation for 24 h (CI measurements every 15 min), 100 µl of the medium was replaced by 80 µl SRM-REC containing 125 ng/ml VEGF-A_{165}. CI was then determined every 2 min for 2 h followed by measurements every 5 min for one day, before 20 µl medium containing nintedanib, ZM323881 or peptide A7R were added. Subsequently, CI was measured every 2 min for 2 h and then every 5 min for additional 24–72 h of cultivation. To study whether nintedanib prevented VEGF-A_{165}-induced CI decrease, CI measurements were done exactly as previously described (Deissler et al., 2017). At the end of each experiment, the integrity of the iBREC monolayer was verified by microscopic examination.

ARPE-19 cells (~10^4 cells in FM) were seeded per well of an E-Plate 96 PET (Acea) and cultivated until a confluent monolayer was reached (four days later; CI ~12), before culture medium was replaced by 200 µl SRM-RPE and CI was measured every 5 min for 24 h. To assess whether VEGF-A_{165} affected the CI of a confluent ARPE-19 monolayer, 100 µl of the medium was substituted by 80 µl SRM-RPE containing 125 ng/ml VEGF-A_{165}, optionally followed by a second addition of 20 µl SRM-RPE with 500 ng/ml VEGF-A_{165} 24 h later. Similar experiments were performed to study the effect of nintedanib: 100 µl of the medium was replaced by 80 µl SRM-RPE containing 25 nM or 250 nM nintedanib for one day, before 20 µl SRM-RPE with or without 500 ng/ml VEGF-A_{165} were added. Alternatively, 20 µl SRM-RPE containing 25 nM or 250 nM nintedanib (with or without 500 ng/ml VEGF-A_{165}) were added to the medium in wells with ARPE-19 cells pre-treated for 1 d with VEGF-A_{165}. The CI was measured consistently every 5 min for up to 100 h after first addition of an effector.

Recorded CI values were normalized in relation to those measured immediately before addition of VEGF-A_{165} or inhibitors as indicated (RTCA Software 2.0) and the results were converted to graphs showing means and standard deviations of at least four individual wells per condition using Graph Pad Prism 6 (Graph Pad Software; San Diego, USA).

2.9. Statistical analyses

To compare measured CI or TEER values at selected time points, values obtained from cell viability assays, or quantified antigen-specific signals of Western blot and immunofluorescence analyses, one-way analyses of variance (ANOVA) followed by Tukey's test to determine differing groups were applied (Graph Pad Prism 6). The nonparametric Wilcoxon signed rank test was used to compare antigen-specific signals of Western blot analyses of effector-treated cells to the hypothetical value of 1.0 of normalized signals from experiments with control cells (Graph Pad Prism 6). Differences resulting in p-values below 0.05 were considered significant. In addition to providing means and corresponding standard deviations, results were presented as scatter plots including this information. All experiments were repeated at least twice with multiple replicates.

3. Results

3.1. Nintedanib prevented VEGF-A_{165}-induced barrier disruption of iBREC

Because inhibition of VEGFR2 by the multi tyrosine-kinase inhibitor tivozanib at 10 nM and the VEGFR2-specific inhibitor ZM323881 at 500 nM completely prevented VEGF-A_{165}-induced barrier disturbance, we assumed a similar impact of nintedanib (Deissler et al., 2017). Disturbing effects on the barrier stability of iBREC that might be caused by exposure to the multi-tyrosine-kinase inhibitor for at least one day were assessed by measuring the cell index (CI) (Fig. 1A) and determining the expression of TJ- and AJ-proteins (data not shown), but these parameters remained unchanged at 10 nM or 100 nM nintedanib. To study whether nintedanib (like tivozanib) blocked VEGF-A_{165}-induced barrier dysfunction of iBREC, cells were pre-treated with 10 nM nintedanib for 2 h, before VEGF-A_{165} was added. In addition to continuous monitoring of the CI, cells were harvested for preparation of cell extracts and subsequent Western blot analyses after 24 h. In accordance with our hypothesis, nintedanib at 10 nM completely prevented the bi-phasic drop of the CI (Fig. 1B) and the decrease of claudin-1 expression typically induced by treatment with VEGF-A (Fig. 1C). Expressed amounts of VEcadherin – resulting in a strong Western-blot band at 130 kDa – were not affected by either VEGF-A_{165} or inhibitors used; smaller fragments indicative of proteolytic cleavage of the protein were not detected (Fig. 1C).

3.2. Nintedanib completely reverted VEGF-A_{165}-induced CI decline of an iBREC monolayer

As other growth factor receptors might be co-activated during extended exposure of the cells to VEGF-A_{165}, we studied whether nintedanib at a concentration of 10 nM where inhibition of other receptor tyrosine kinases despite of VEGFR2 is rather unlikely, is also sufficient to *revert* VEGF-A_{165}-induced reduction of the CI. iBREC were exposed to VEGF-A_{165} for one day before nintedanib was added at 10 nM or 100 nM and the CI was recorded for up to three days. The lowered CI significantly increased shortly after addition of 10 nM nintedanib and within 12 h reached normal values which were stable at least for three days (Fig. 2A); a concentration of 100 nM was slightly less efficient (Fig. 2B). In accordance with our observation that 10 nM tivozanib likely blocking only VEGFR2 (data not shown) also completely reverted the VEGF-A_{165}-induced drop of the CI, these findings further emphasized the crucial role of the VEGFR2. To test this hypothesis, similar experiments were performed with the VEGFR2-specific inhibitor ZM323881 and, accordingly, this compound also completely reverted a VEGF-A_{165}-induced CI drop in a process beginning shortly after its addition (Fig. 2C). The CI started to decline again several hours later in accordance with our previous observation that ZM323881 has a limited stability under conditions of cell cultivation (Deissler et al., 2017).

3.3. Nintedanib reverted VEGF-A_{165}-induced changes of iBREC TJ and AJ compositions

We also investigated if nintedanib completely reverted VEGF-A_{165}-

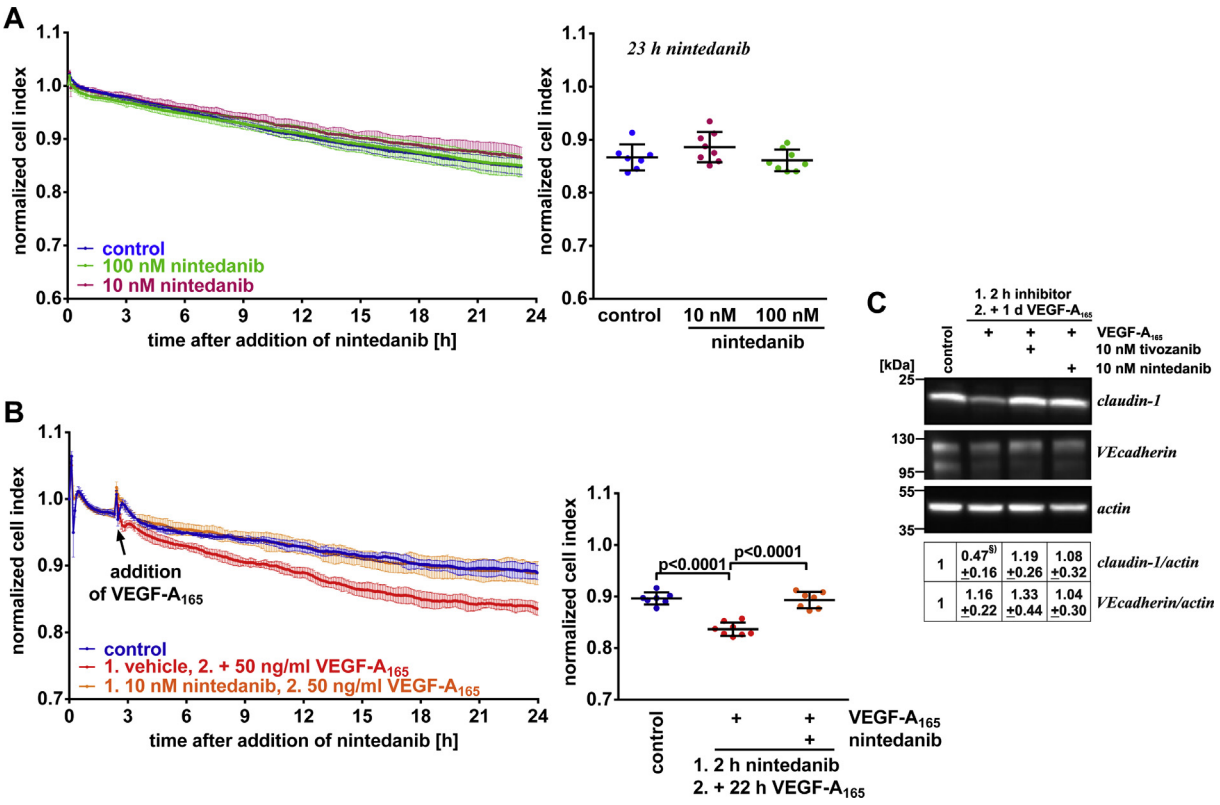

Fig. 1. Blocking VEGFR2 with nintedanib completely prevented response of iBREC to VEGF-A_{165}. (A) CI values were determined continuously as measures of barrier function of confluent iBREC exposed to nintedanib, which had no effect at concentrations of 10 or 100 nM. (B) Confluent iBREC kept in SRM-REC for 24 h were pre-treated with 10 nM nintedanib for 2 h before 50 ng/ml VEGF-A_{165} was added and the CI was monitored for additional 24 h. Short- and long-term effects of VEGF-A_{165} were completely blocked by 10 nM nintedanib. CI values were normalized in relation to those measured immediately before addition of nintedanib. Means and standard deviations obtained from at least seven individual wells are shown; statistical analysis was performed at indicated time points after addition of nintedanib as described in Materials and Methods. (C) Cells treated with nintedanib, tivozanib and VEGF-A_{165} as described in (B) were harvested for preparation of cell extracts and subsequent Western blot analyses. VEGF-A_{165}-induced reduction of claudin-1 expression was prevented by inhibition of VEGFR2 with 10 nM nintedanib or tivozanib. Signals were normalized as described in Materials and Methods, n = 5 for each condition. §) $p < 0.006$ compared to control or inhibitors.

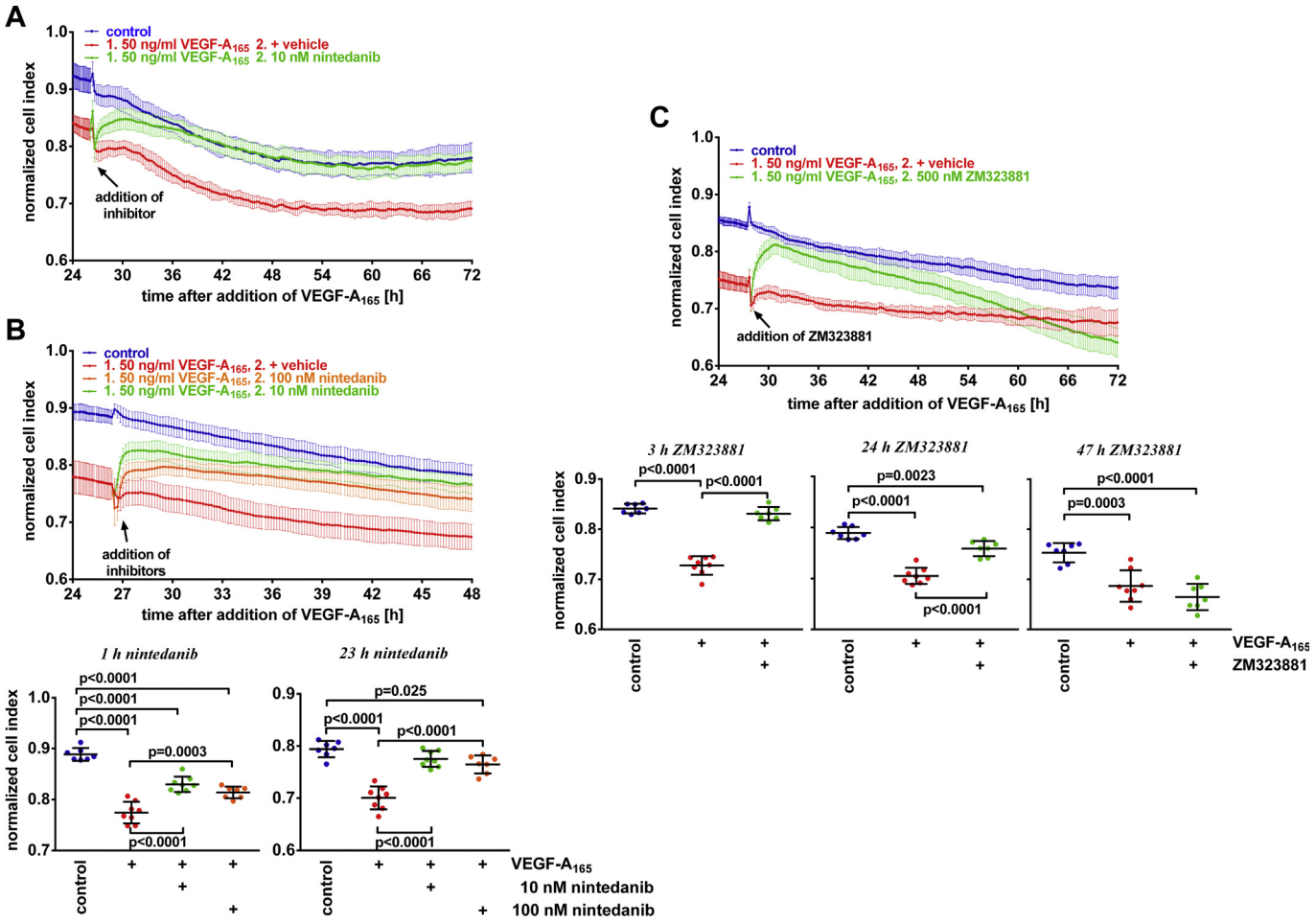

Fig. 2. Blocking VEGFR2 with nintedanib or ZM323881 reverted VEGF-A_{165}-induced CI reduction of iBREC monolayers. iBREC were pre-treated with 50 ng/ml VEGF-A_{165} for one day before (A, B) nintedanib or (C) ZM323881 were added and the CI was recorded as indicated. In all experiments, CI values were normalized in relation to those measured immediately before addition of VEGF-A_{165}. Data obtained from at least seven individual wells are presented as means and standard deviations and statistical analyses were performed at indicated time points after addition of the inhibitors as described in Materials and Methods. (A) VEGF-A_{165}-induced CI reduction was completely reverted after addition of 10 nM nintedanib and this normalization was stable for at least three days. (B) Higher concentrations of nintedanib were not superior. (C) The effect of 500 nM ZM32388 was comparable to nintedanib during the first 24 h but declined after prolonged exposure (see also Fig. 5 A).

induced loss of claudin-1 by treating iBREC exposed to VEGF-A_{165} with nintedanib for one or two days. Subsequent Western blot analyses of whole cell extracts revealed that VEGF-A_{165}-treaed iBREC needed to be exposed to the VEGFR2 inhibitor (10 nM nintedanib) for two days to completely regain claudin-1 (Fig. 3A). Additional blocking of other protein kinases by increasing the concentration of nintedanib to 100 nM was not superior (Fig. 3A). Exposure to ZM323881 for one day only partly, although significantly re-instated claudin-1 (Fig. 3B), but longer incubation times were not more efficient due to its limited stability (data not shown). The slightly higher expression of claudin-5 caused by VEGF-A_{165} was also reverted by nintedanib or ZM323881, although the effects did not reach statistical significance; expression of VEcadherin remained unchanged throughout the experiments (Fig. 3).

Treatment of iBREC with VEGF-A_{165} for one day led to loss of claudin-1 from the plasma membrane which was completely reverted by treating the cells with 10 nM nintedanib for one day (Fig. 4). Only subtle and less obvious changes of the strong plasma membrane localization of claudin-5 and VEcadherin were induced by exposure to VEGF-A_{165}: The staining of the plasma membrane detected by immunofluorescence was uneven and partly interrupted (Fig. 4, yellow arrows). These changes were also no longer present after subsequent treatment with 10 nM nintedanib.

3.4. Additional blocking of non-tyrosine kinase receptor NRP-1 was not superior to revert VEGF-A_{165}-induced dysfunction of the iBREC barrier

ZM323881 only transiently prevented and reverted the VEGF-A-induced decline of the CI (Fig. 2C) and only partly re-instated lost claudin-1 expression one day after its addition to VEGF-A-exposed iBREC (Fig. 3B; Deissler et al., 2017). As VEGF-A_{165} also binds to and thereby activates NRP-1, additional inhibition of this receptor might be an advantage (Oh et al., 2002; Pan et al., 2007). To test this hypothesis, we used the peptide A7R which specifically binds to the non-tyrosine kinase receptor and blocks VEGF-A-dependent migration and proliferation of human macrovascular EC of the umbilical cord (Tirand et al., 2006; Starzec et al., 2006). However, this peptide neither reverted the VEGF-A-induced CI drop (Fig. 5A) or low expression of claudin-1 (Fig. 5B) on its own nor enhanced the effect of ZM323881.

3.5. VEGF-A_{165}, but not nintedanib differently affected metabolic activity of short- or long-term cultivated ARPE-19 cells

VEGF-A is secreted by RPE cells *in vitro* and *in vivo*, and exogenously added surplus amounts of growth factor as well as inhibition of its receptors might affect vital characteristics of ARPE-19 cells (Ford et al., 2011; Ford and D'Amore, 2012; Klettner et al., 2013). The response of

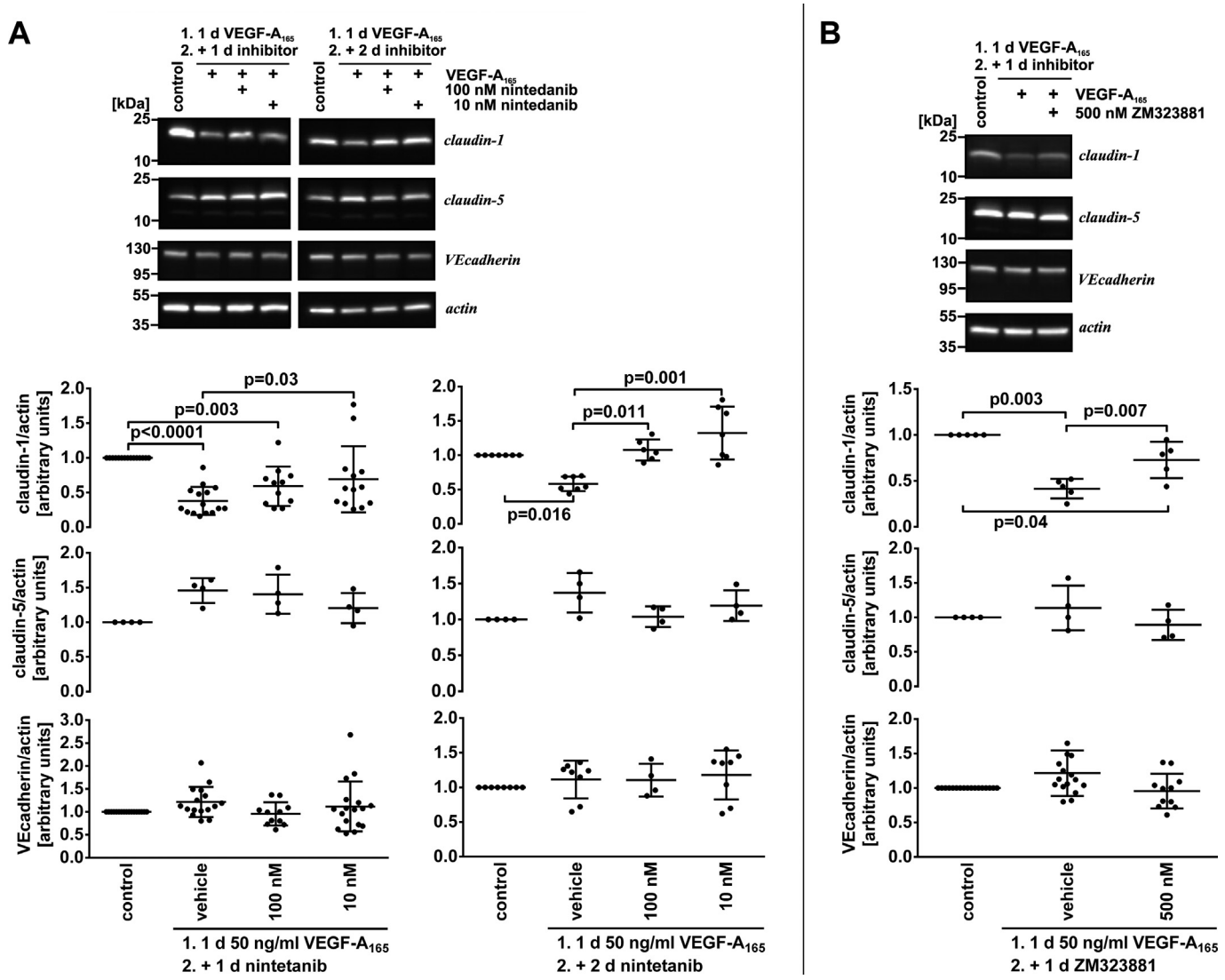

Fig. 3. Blocking VEGFR2 with nintedanib or ZM323881 reverted VEGF-A_{165}-induced loss of claudin-1 expressed by iBREC. Confluent iBREC were kept in serum-reduced culture medium for one day and treated with 50 ng/ml VEGF-A_{165} for additional 24 h. Inhibitors were then added and after one or two days cells were harvested for preparation of cell extracts to be analyzed by Western-blot. (A) Expression of claudin-1 was lower after VEGF-A_{165}-treatment, but significantly increased after exposure of the cells to 10 nM nintedanib for one day and reached normal values after two days. Treatment with VEGF-A_{165} resulted in a slightly increased expression of claudin-5, which readjusted to normal levels after addition of inhibitors (differences not statistically significant); expression of VEcadherin was not significantly affected. Results obtained with 10 nM or 100 nM nintedanib were similar. (B) VEGF-A_{165}-induced changes of claudin-1 and claudin-5 expression were reverted by 500 nM ZM323881 although the measured claudin-5 differences were not statistically significant; presence of VEcadherin was not significantly changed by the effectors. Normalization of signals and statistical analyses of data were performed as described in Materials and Methods.

these cells likely also depends on the time of cultivation which was shown to correlate with the degree of their polarization (Dunn et al., 1996, 1998; Kannan et al., 2006; Geisen et al., 2006; Miyamoto et al., 2007; Ablonczy et al., 2011; Ford and D'Amore, 2012). During the first week of cultivation on laminin-coated porous membrane inserts, the ARPE-19 cells only had a very low TEER of ~4 Ωcm^2 (Fig. 6A) accompanied by weak expression of the TJ-protein ZO-1 (Fig. 6B), indicative of a poor barrier function. From the second week onwards, the TEER increased significantly reaching values of ~20 Ωcm^2 at day 10 ($p = 0.0008$, compared to day one). Upon prolonged cultivation of ARPE-19 cells, plasma membrane localization of substantial amounts of ZO-1 became evident, most prominently between days 21–27 of cultivation (Fig. 6B). During the same time the TEER increased significantly further, reaching a maximum of ~45 Ωcm^2 (Fig. 6A), which is of a similar range previously reported (Ablonczy and Crosson, 2007; Dunn et al., 1996; Geisen et al., 2006). To assess modulating effects of VEGF-A_{165} or putative cytotoxic effects of nintedanib, short- or long-term cultivated ARPE-19 cells were exposed to increasing concentrations of the effectors for one day before enzymatic activities of NAD(P)H-dependent oxidoreductases were determined. VEGF-A_{165} significantly stimulated the metabolic activity of short-term cultivated ARPE-19 cells (Fig. 6C) but that of long-term cultivated ones decreased during exposure (Fig. 6D). Nintedanib was well tolerated by ARPE-19 cells, regardless of cultivation time, at concentrations sufficient for specific inhibition of VEGF, PDGF and FGF receptors but strongly affected the cells at higher concentrations (Fig. 6C and D).

3.6. Nintedanib and VEGF-A_{165} did not change the CI of short-term cultivated ARPE-19 cells

Because treatment with VEGF-A_{165} or nintedanib might also change the albeit weak barrier properties of short-term cultivated ARPE-19 cells, we determined the CI of a confluent monolayer cultivated on E-Plates for 4 day as an indicator of their permeability. In contrast to

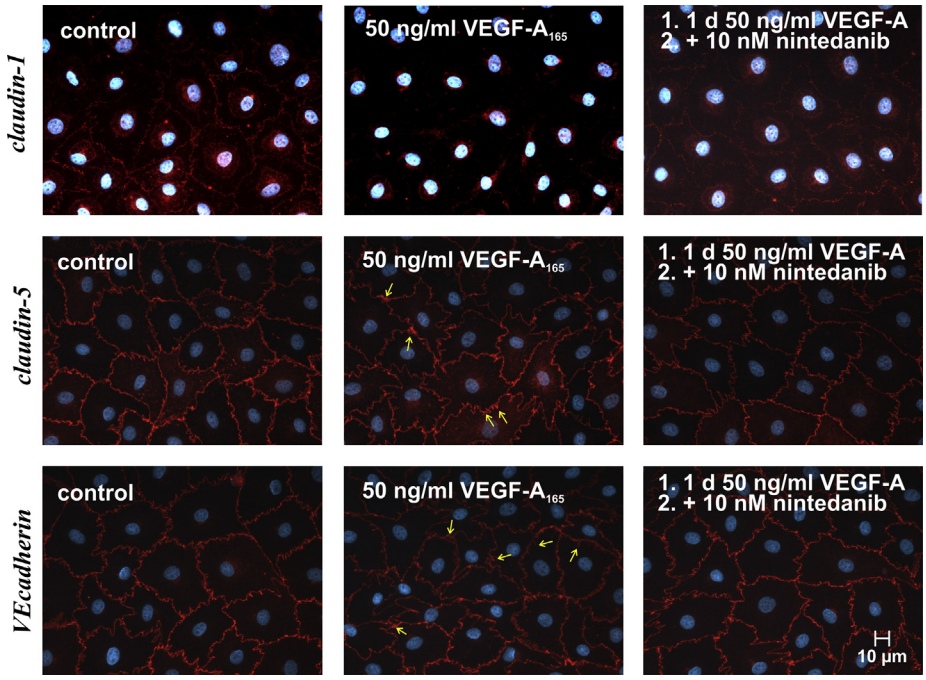

Fig. 4. Blocking VEGFR2 with nintedanib reverted VEGF-A_{165}-induced effects on junction proteins of iBRECAfter exposing confluent iBREC to $VEGFA_{165}$ for one day, 10 nM nintedanib was added and cells were fixated two days later. TJ-proteins claudin-1 and claudin-5 as well as AJ-protein VEcadherin were localized by immunofluorescence staining. Nintedanib at 10 nM completely reverted VEGF-A_{165}-induced disappearance of plasma membrane staining specific for claudin-1. Treatment of iBREC with VEGF-A_{165} resulted in slightly more uneven and interrupted plasma membrane stainings (yellow arrows) of VEcadherin and claudin-5; these very subtle effects were also reverted by VEGFR2 inhibition with 10 nM nintedanib. (For interpretation of the references to colour in this figure legend, the reader is referred to the Web version of this article.)

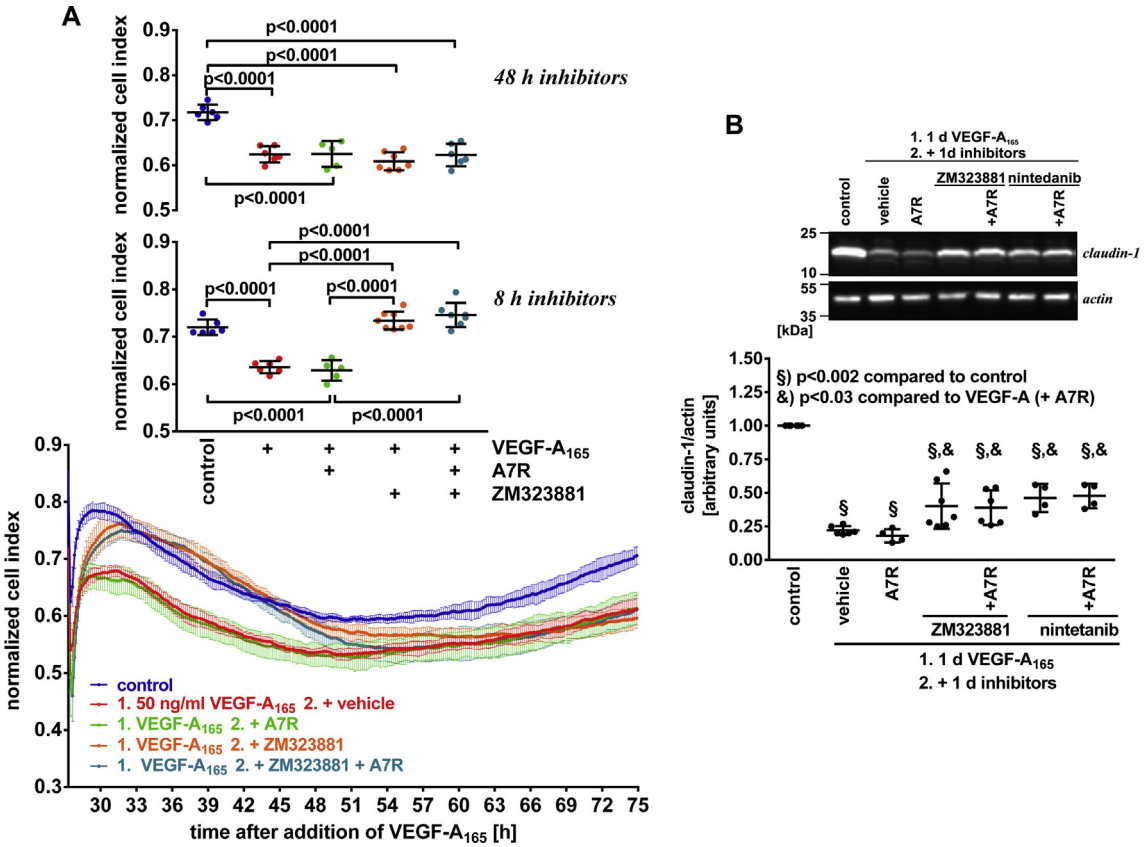

Fig. 5. Additional inhibition of NRP-1 was not superior to revert VEGF-A-induced barrier dysfunction. (A) After exposure of iBREC with 50 ng/ml VEGF-A_{165} for one day, 500 nM ZM323881, 50 µM A7R or a combination of both were added and the CI was recorded as indicated. CI values were normalized in relation to those measured immediately before addition of VEGF-A_{165}. Data obtained from at least five individual wells are shown as means and standard deviations and statistical analyses at 8 h and 48 h after addition of inhibitors were performed as described in Materials and Methods. ZM323881 efficiently, but transiently reverted the VEGF-A-induced low CI but addition of the inhibitor of NRP-1 A7R, which did not have any effect on its own, was not superior. (B) 500 nM ZM323881, 10 nM nintedanib, 50 µM A7R or combinations thereof were added to iBREC exposed to VEGF-A_{165} for one day before cells were harvested one day later for preparation of cell extracts followed by Western blot analyses. A7R on its own did not change the low level of claudin-1 induced by VEGF-A_{165}, and combination of A7R and ZM323881 or nintedanib re-instated claudin-1 similarly compared to the VEGFR-inhibitors alone. Normalization of signals and statistical analyses of data were performed as described in Materials and Methods.

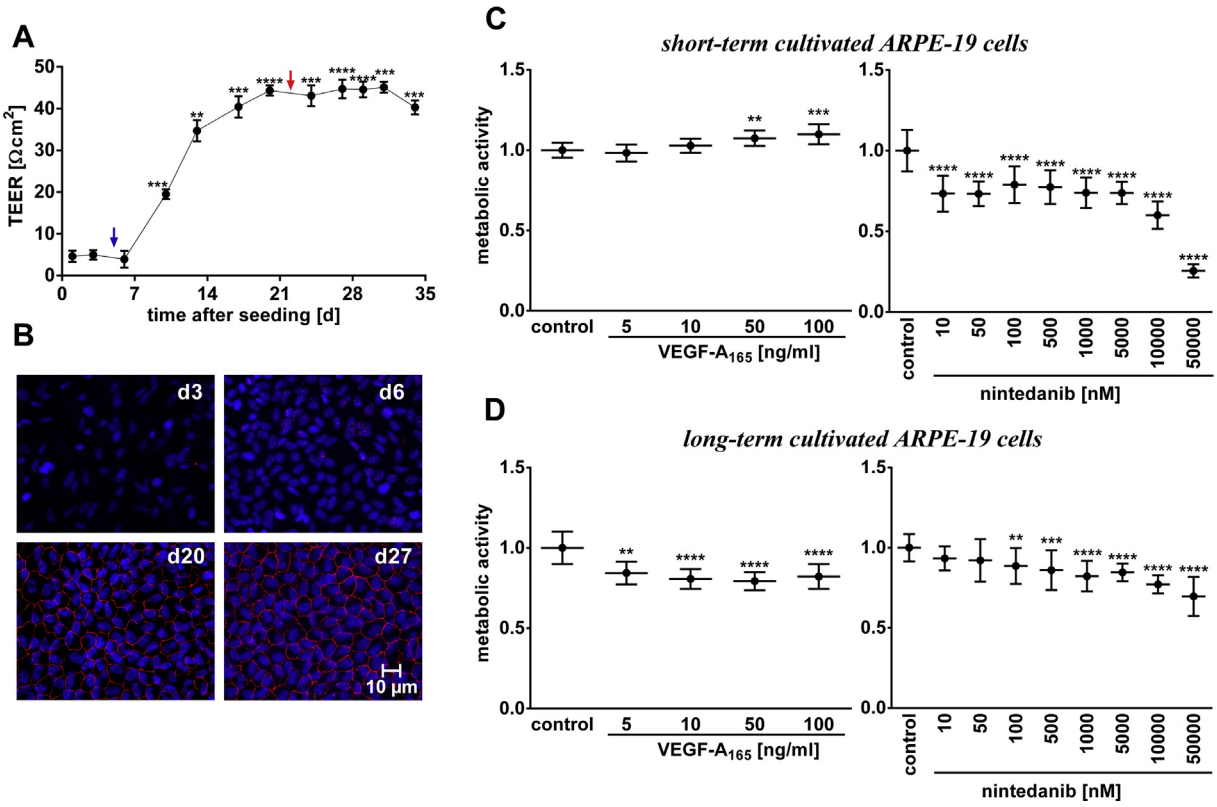

Fig. 6. VEGF-A_{165} and nintedanib affected metabolic activity of short- or long-term cultivated ARPE-19 cells in different ways. (A, B) ARPE-19 cells were cultivated on porous membrane inserts for up to four weeks and (A) the TEER was measured every few days or (B) expression of ZO-1 was assessed by immunofluorescence staining at given time points. Strong expression of ZO-1 clearly correlated with an increase and stabilization of the TEER. At the start of cell index measurements (see Fig. 7), marked by the blue arrow, expression of ZO-1 and the TEER were both still extremely low. The red arrow indicates the start of exposure of the long-term cultivated ARPE-19 cells to VEGF-A_{165}, followed by addition of nintedanib (see Fig. 8). **) $p < 0.01$, ***) $p < 0.001$, ****) $p < 0.0001$ compared to values measured on day one. Means and standard deviations of data obtained from four replicates are shown and statistical analyses were performed as described in Materials and Methods. (C, D) Metabolically active (C) short- or (D) long-term cultivated ARPE-19 cells were determined after their exposure to increasing concentrations of either VEGF-A_{165} or nintedanib for 1 day as described in Materials and Methods. After treatment with the growth factor, short-term cultivated ARPE-19 cells were metabolically more active, whereas long-term cultivated cells were less active. ARPE-19 cells tolerated nintedanib up to 1 µM (short-term cultivated) or 5 µM (long-term cultivated), respectively. **) $p < 0.01$, ***) $p < 0.001$, ****) $p < 0.0001$ compared to control. Means and standard deviations of data obtained from ten replicates are shown and statistical analyses were performed as described in Materials and Methods. (For interpretation of the references to colour in this figure legend, the reader is referred to the Web version of this article.)

discontinuous TEER measurements, continuous monitoring of the CI allows the detection of subtle and transient changes even if the barrier is as weak as that formed by these cells. In general, additional 50 ng/ml VEGF-A_{165} stabilized the CI and this was even more pronounced after addition of a second portion of the growth factor (Fig. 7A). Therefore, blocking the VEGF receptors might be harmful for ARPE-19 cells in early stages of cultivation but inhibition by nintedanib was not sufficient to affect their CI (Fig. 7B). Addition of 10 nM or 100 nM nintedanib to the cells pre-treated with VEGF-A_{165} for 24 h also did not significantly change the CI in experiments with (Fig. 7D) or without (Fig. 7C) further addition of the growth factor.

3.7. Nintedanib reversed VEGF-A_{165}-induced decline of TEER and loss of TJ protein ZO-1 from plasma membranes of long-term cultivated ARPE-19 cells

Short-term cultivation of ARPE-19 cells most likely does not properly reflect the phenotype of the polarized RPE *in vivo* and these cells presumably respond to VEGF-A or inhibitors of its receptors in a different way. Therefore, ARPE-19 cells established by prolonged cultivation on laminin-coated porous membrane inserts were treated with VEGF-A_{165} for one day before addition of nintedanib and subsequent TEER measurements to determine potential effects on the barrier. Exposure to the growth factor resulted then in a significant decrease of the TEER from 42 ± 2 Ωcm² to 31 ± 1 Ωcm² ($p = 0.012$; Fig. 8A). This drop was completely reverted by 10 nM and 100 nM nintedanib to TEER values of 44 ± 4 Ωcm² and 41 ± 2 Ωcm², respectively which were not different from those measured for control cells (42 ± 3 Ωcm²; Fig. 8A). The lower concentration of the inhibitor itself slightly, but not significantly increased the TEER (49 ± 1 Ωcm²; $p = 0.14$; Fig. 8B). Accordingly, VEGF-A_{165}-reduced amounts of ZO-1 in the plasma membrane were completely normalized by addition of nintedanib which as single effector significantly increased expression of the TJ-protein at the plasma membrane; effects of higher nintedanib concentrations were not more pronounced (Fig. 8C).

3.8. Nintedanib decreased secretion of VEGF-A by long-term cultivated ARPE-19 cells

Activation or inhibition of VEGFRs might change secretion of VEGF-A by long-term cultivated ARPE-19 cells. After exposure of the cells grown on membrane inserts to 50 ng/ml VEGF-A_{165} for one day, the culture medium was completely exchanged with growth factor-free culture medium with or without nintedanib and the supernatant taken from the apical chamber 24 h later was analyzed for the presence of VEGF-A. Prior exposure to VEGF-A did not change the amount of VEGF-A secreted by these cells during 24 h (59 ± 6 pg versus 62 ± 6 pg; $p = 0.93$), but after subsequent treatment with 10 nM nintedanib it was significantly lower (31 ± 4 pg, $p < 0.0001$); a similar effect was

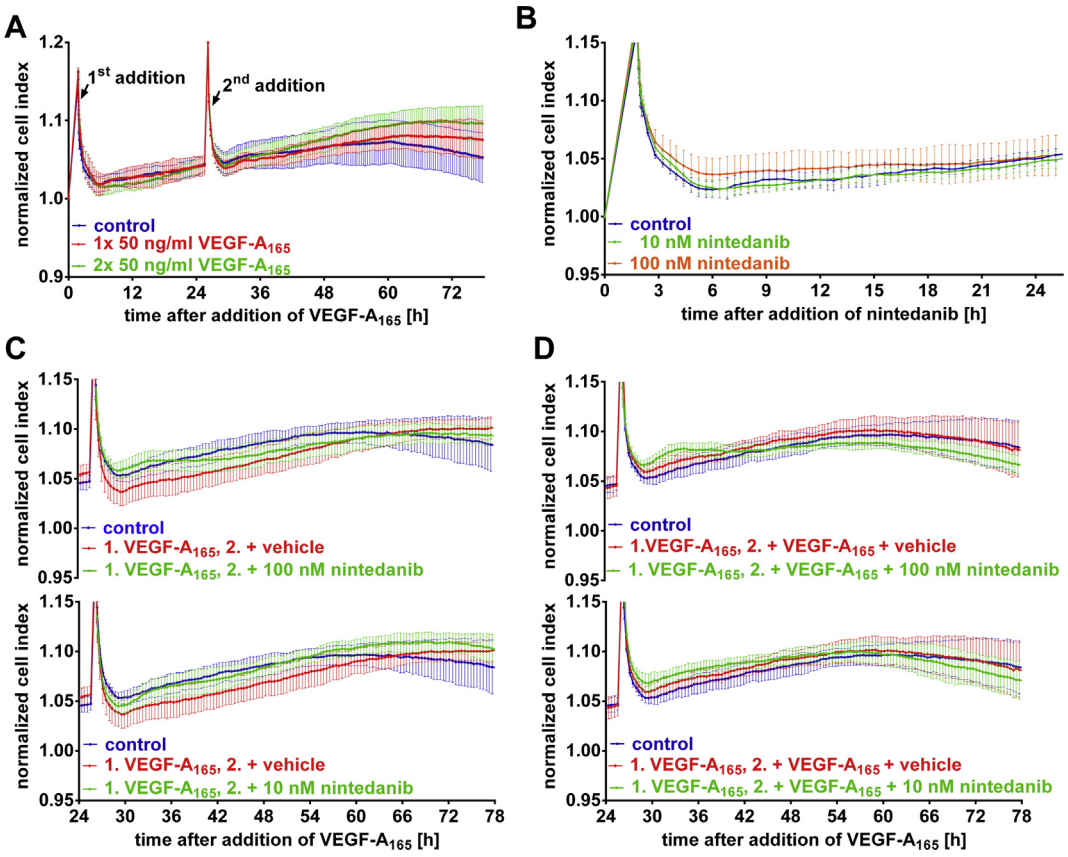

Fig. 7. Nintedanib did not alter barrier function of short-term cultivated ARPE-19 cells in the presence of VEGF-A_{165}. (A, B) Confluent ARPE-19 cells cultivated on gold electrodes for four days (see blue arrow in Fig. 6) were exposed to (A) VEGF-A_{165} (one or two additions) or to (B) nintedanib and the CI as a measurement of their barrier function was continuously recorded. The growth factor slightly increased the CI especially after two consecutive additions whereas the inhibitor of VEGFR1/2 did not noticeably change the barrier properties of short-term cultivated ARPE-19 cells. (C, D) After exposure of the confluent cells to 50 ng/ml VEGF-A_{165} for one day, (C) nintedanib or (D) the inhibitor together with 50 ng/ml VEGF-A_{165} were added and the CI was measured continuously. The CI only slightly changed under either condition; the effects of 10 and 100 nM nintedanib were similar. CI values were normalized in relation to those measured immediately before addition of VEGF-A_{165} (A, C, D) or nintedanib (B) and data obtained from four individual wells are shown as means and standard deviations. (For interpretation of the references to colour in this figure legend, the reader is referred to the Web version of this article.)

observed with 100 nM nintedanib (28 ± 4 pg, $p < 0.0001$).

4. Discussion

Impaired VEGF-A-triggered signaling plays an important role in the development of severe ocular diseases of which neovascularization in the choroid or retina as well as dysfunction of the inner and outer blood-retina barrier are typical characteristics (Aiello et al., 1994; Ambati et al., 2003; Campochiaro 2000, 2013; Kliffen et al., 1997; Qaum et al., 2001). Here we investigated whether inhibition of the VEGFR2 is sufficient to completely revert changes induced by VEGF-A_{165} in the major cell types of the inner or outer blood-retina barrier. We also studied potential compromising effects of VEGFR2 inhibition on RPE cells because they express significant amounts of VEGF-A and therefore blocking its signaling might be harmful under certain circumstances (Byeon et al., 2010; Ford et al., 2011; Klettner et al., 2013; Ranjbar et al., 2016b).

To analyze consequences of interference with VEGFR2 function for immortalized endothelial cells of the bovine retina (iBREC) as a well-accepted model of the inner blood-retina barrier, these cells were exposed to VEGF-A_{165} and subsequently to the well-characterized inhibitors nintedanib, tivozanib and ZM323881 (Deissler et al., 2005, 2011; 2013a; Hilberg et al., 2008; Nakamura et al., 2006; Whittles et al., 2002). Chosen concentrations (10 nM nintedanib/tivozanib: inhibition of VEGFR2; 100 nM nintedanib/tivozanib: additional inhibition of VEGFR1 and other receptor tyrosine kinases; 500 nM ZM323881: inhibition of VEGFR2 only) allowed most specific inhibition of the receptor(s) targeted in the experiments. The cell index was assessed as a measure of permeability, and expression as well as localization of the TJ-protein claudin-1 as a marker of a functional iBREC barrier (Deissler et al., 2008, 2011, 2013a, 2017). Continuous determination of the CI of cells cultivated on gold electrodes is an excellent, nearly non-invasive technique that allows the detection of transient and even subtle changes of barrier properties of cell monolayers. By using this highly sensitive method it is possible to recognize changes of paracellular and transcellular flow, and of adhesion through cell-matrix interactions (Sun et al., 2012). However, due to the limited stability of the gold electrodes, extended measurements are restricted to a period of ten days.

VEGF-A_{165} induced a long-lasting reduction of the CI of iBREC which could be completely reverted by subsequent treatment with nintedanib or tivozanib. Notably, these inhibitors at concentrations very likely solely suppressing the activity of VEGFR2 and the VEGFR2-specific inhibitor ZM323881 were similarly efficient, indicating that blocking the activities of VEGFR1 and other receptor tyrosine kinases like FGFRs or PDGFRs seems not to be necessary. These results are in accordance with our previous findings that barrier dysfunction, proliferation and migration of iBREC, are all promoted by VEGF-E, which binds and activates VEGFR2 and NRP-1, whereas the ligand of VEGFR1 placental growth factor (PlGF) only stimulated their proliferation (Deissler et al., 2013a, 2013b). Similarly, suppressing interaction of the growth factor with its receptor(s) by the VEGF-A-specific Fab fragment

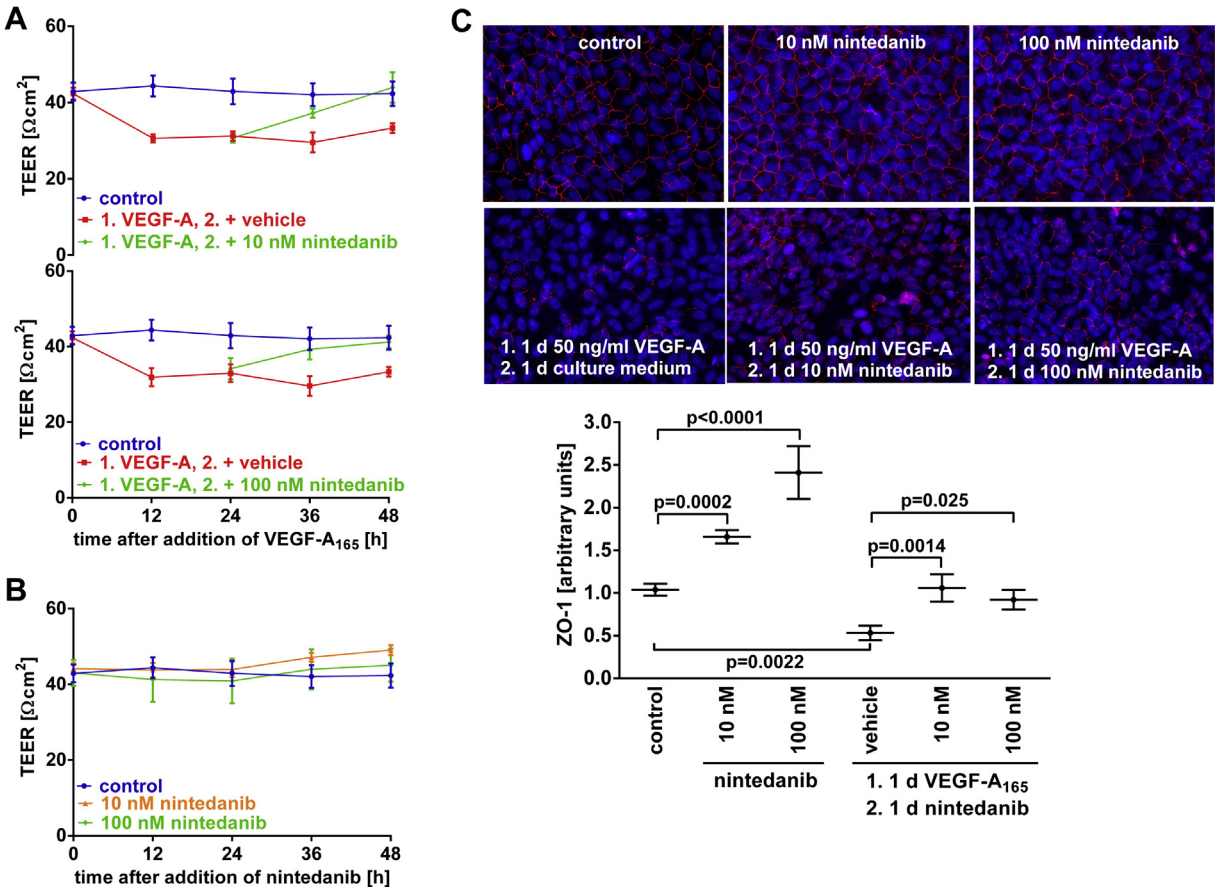

Fig. 8. Decreased TEER and lower ZO-1 expression of long-term cultivated ARPE-19 cells induced by VEGF-A_{165} were both reverted by nintedanib. ARPE-19 cells were cultivated on porous membrane inserts until a stable TEER and strong expression of ZO-1 were observed (~21 d, see Fig. 6A, red arrow). Cells were then exposed at their apical side (A, C) to VEGF-A_{165} for 24 h followed by 10 nM or 100 nM nintedanib or (B, C) to the inhibitors only. (A, B) TEER was measured or (C) cells were fixated for immunofluorescence staining of the TJ-protein ZO-1 one day later; fluorescence signals were normalized and calculated as described in Materials and Methods. Data obtained from at least three replicates are presented as means and standard deviations; statistical analyses were performed as described in Materials and Methods. Nintedanib (10 nM and 100 nM) stabilized the TEER and expression of ZO-1 at the plasma membrane. TEER and amounts of ZO-1 were significantly reduced by VEGF-A_{165} but reached normal values one day after addition of nintedanib (10 nM or 100 nM). (For interpretation of the references to colour in this figure legend, the reader is referred to the Web version of this article.)

ranibizumab was also sufficient to completely revert barrier disturbance of these cells: Barrier normalization was achieved even in the presence of other growth factors such as basic FGF, insulin-like growth factor 1, P*l*GF and/or VEGF-B (Deissler et al., 2011, 2013a, 2015). In accordance, basic FGF neither affected the function of an established iBREC barrier nor modulated the disturbing effect of VEGF-A despite its ability to stimulate proliferation and migration of the cells (Deissler et al., 2005, 2011, 2013b). It is also of interest in this context that additional blocking of the PDGFRs by increasing the concentration of nintedanib did not improve the recovery of a VEGF-A-deranged iBREC barrier, however, PDGF isoforms also did not modulate the CI of an unchallenged or VEGF-A-challenged iBREC monolayer suggesting that these cells lack PDGF-induced signal transduction. Therefore, additional blocking of FGFRs or PDGFRs seems not to be advantageous in approaches to stabilize the REC barrier although dual inhibition of FGFR and VEGFR has been proven to be superior in blocking angiogenesis, and inhibition of PDGFRs suppressed pathological retinal neovascularization in a murine model of oxygen-induced retinopathy confirming again different cellular mechanisms underlying neovascularization and barrier dysfunction (Stahl et al., 2009; Li et al., 2016; Zhou et al., 2018). In addition to activation of the VEGFR2 by VEGF-A_{165}, bridging with non-tyrosine kinase receptor NRP-1 has been described to be relevant for regulation of EC migration (Oh et al., 2002; Pan et al., 2007). However, NRP-1-mediated signal transduction most likely plays only a minor role in VEGF-A-induced barrier disturbances because otherwise additional blocking of this receptor should have enhanced the effect of VEGFR2-inhibitor ZM323881. This hypothesis is supported by our previous observation that the shorter splice variant VEGF-A_{121} which only weakly interacts with NRP-1, induces barrier dysfunction of iBREC without stimulating their migration (Deissler et al., 2008, 2013a; Pan et al., 2007). These results clearly point to a role of NRP-1 in concert with VEGFR2 in the regulation of migration of iBREC, whereas an involvement in the control of barrier function seems unlikely.

Interestingly, barrier function of iBREC was completely normal again one day after addition of nintedanib although expression of claudin-1 reached normal levels only after extended exposure for two days in accordance with previous observations (Deissler et al., 2011). Obviously, a lower total amount of the TJ-protein is sufficient to ensure proper barrier function, and indeed a considerable claudin-1 staining was already seen at the plasma membrane one day after addition of the inhibitor. That VEGF-A_{165} very subtly changed the plasma membrane localizations of claudin-5 and VEcadherin - effects also completely reversible by subsequent VEGFR2 inhibition - were consistent with our previous findings and those of others (Deissler et al., 2008, 2017; Suarez et al., 2014; Jeong et al., 2016; Kim and Suh, 2017).

Responses of ARPE-19 cells to either VEGF-A_{165} or inhibitors of its receptors were strongly dependent on their cultivation time. Short-term cultivated ARPE-19 cells are characterized by a low expression and secretion of VEGF-A, patchy and weak expression of ZO-1 at the plasma

membrane, and a low TEER (Ablonczy et al., 2011; Ford and D'Amore, 2012). Therefore, assessment of potential effects of the effectors investigated on a confluent monolayer of these cells required a highly sensitive method like measuring the cell index. VEGF-A_{165} not only slightly increased the cell index of a confluent monolayer of short-term cultivated ARPE-19 cells but also stimulated their metabolic activity which was significantly decreased only by extremely high concentrations of nintedanib, suggesting rather negligible toxicity of this substance. The inhibitor also did not affect the barrier properties of the cells as the cell index and the patchy and weak expression of ZO-1 at the plasma membrane remained unchanged. This clearly indicates that by targeting the receptor tyrosine kinases VEGFR1 or VEGFR2 the - albeit weak - barrier function as well as the viability of short-term cultivated ARPE-19 cells cannot be diminished, which is somehow surprising as they express considerable amounts of VEGF-A (Ford et al., 2011). However, the barrier properties at this stage might be too weak to measure any effect. In strong contrast to its effect on non-polarized cells, addition of VEGF-A_{165} to long-term cultivated ARPE-19 cells considerably lowered their increased TEER. Strong expression of ZO-1 at the plasma membrane, typically emerging during prolonged cultivation of ARPE-19 cells on laminin-coated permeable membrane inserts, also declined significantly as a consequence of treatment with VEGF-A_{165} (Kannan et al., 2006, Fig. 8B). Regarding both reduced TEER - determined as a measure of barrier function - and loss of ZO-1, subsequent treatment with nintedanib resulted in complete normalization of the cells. These results, similar to that from experiments with iBREC, strongly support the assumption that signaling involved in the induction of barrier dysfunction of long-term cultivated ARPE-19 cells by VEGF-A_{165} is mediated predominantly by VEGFR2. In accordance with our finding, Ablonczy and Crosson (2007) observed that VEGFR2-binding VEGF-E, but not the VEGFR1 agonist P*l*GF increased the permeability of polarized ARPE-19 cells. Moreover, they showed that VEGF-E-induced higher permeability of RPE cells was abolished by pretreatment with the VEGFR2 inhibitor ZM323881. The observed striking differences between short- and long-term cultivated ARPE-19 cells are in complete accordance with previous observations of different responses of these variants to various effectors (Ford et al., 2011; Ford and D'Amore, 2012). Therefore, it is an obvious conclusion that results relevant to the physiological situation can only be obtained with long-term cultivated ARPE-19 cells.

The use of the intriguing cell line ARPE-19 as an *in vitro* model for RPE has been discussed controversially in recent years. Derived postmortem from the RPE cell layer of a human eye, it demonstrates many of the properties of native RPE cells such as cobblestone morphology, establishment of a monolayer, polarization when cultured on porous supports, expression of proteins specific for RPE and establishing tight junctions (Dunn et al., 1996, 1998; Ford and D'Amore, 2012). On the other hand, the cells are hypersensitive to the effects of VEGF-variants, express little or no pigmentation, and the barrier formed by TJs of ARPE-19 cells is considerably weaker compared to that of primary RPE cells (Ablonczy et al., 2011). Therefore, it has been suggested that ARPE-19 cells resemble the RPE of aged or diseased eyes. It is also of interest, that cultures of ARPE-19 cells contain immortal as well as mortal cells; the latter are highest in cultures of cells below sixty population doublings - as used in our experiments - and therefore representative of native RPE cells (Kozlowski, 2015).

Expression and secretion of VEGF-A by ARPE-19 cells increases with their extended cultivation on porous membranes, correlating with appearance of strongly increased amounts of the TJ-proteins occludin and ZO-1 at the plasma membrane (Ford et al., 2011; Ford and D'Amore, 2012). In accordance with the observation that secretion of VEGF-A by primary porcine RPE cells decreased during inhibition of VEGFR by SU1498, nintedanib exhibited a similar effect on long-term cultivated ARPE-19 cells, suggesting autocrine or paracrine regulation of VEGF-A by this cell type (Klettner et al., 2013). Interestingly, blocking VEGF-induced signaling by inhibiting the tyrosine kinase activity with nintedanib did not change barrier properties of long-term cultivated ARPE-19 cells, whereas the VEGF-A-binding IgG bevacizumab which interferes with the interaction of the growth factor and its receptor, slightly increased permeability of primary porcine RPE cells and affected viability of polarized ARPE-19 cells although long-term cytotoxic effects of bevacizumab were not observed (Miura et al., 2010; Ford et al., 2011; Schottler et al., 2018). On the basis of our results, one might speculate that inhibiting VEGF-signaling is per se not fatal for VEGF-A-expressing RPE cells and that the differing effects of bevacizumab on RPE cells, e.g. decreased phagocytotic activity, changed microvilli structures, and an increased portion of apoptotic cells, might well be due to the nature of the VEGF-inhibiting protein of which high, non-physiological amounts were found in the cells (Klettner et al., 2010; Miura et al., 2010; Ford et al., 2011; Ranjbar et al., 2016a, 2016b). In accordance with this assumption, insensitivity to inhibition of the VEGFRs by prolonged exposure to a high dose of SU4312 was observed in experiments with retinal ganglion cells and photoreceptors although endogenous VEGF is important for their survival (Saint-Geniez et al., 2008; Miki et al., 2010).

Considering the high clinical relevance of therapeutic VEGF inhibition, it is of particular interest that additional blocking of other growth factor receptors like FGFRs or PDFGRs, appears not to be necessary to efficiently revert a VEGF-A_{165}-induced barrier dysfunction of the cells of the inner and outer BRB. This hypothesis is supported by previous observations that inhibition of VEGFR2 is also sufficient to prevent VEGF-A_{165}-induced barrier disturbance of monolayers formed by both cell types, REC and RPE cells (Ablonczy and Crosson, 2007; Deissler et al., 2017). Extended treatment with VEGF-A_{165} might result in activation of additional signal transduction pathways, but concerning the regulation of barrier function of REC and RPE cells, this seems to play a minor role, in contrast to angiogenic processes in which synergistic effects of growth factor actions have been described (Castellon et al., 2002; Deissler et al., 2011, 2013b; Li et al., 2016; Stahl et al., 2009). Dual VEGF-A and PDGF-BB/AB antagonists were also not superior to anti-VEGF monotherapy with regard to visual acuity which strongly depends on the severity of macular edema determined by the degree of leakage through the inner as well as outer blood-retina barrier (Dunn et al., 2017).

5. Conclusions

The results of our study based on *in vitro* models of both blood-retina barriers not only provide a rationale for clinical observations but by confirming that vital properties of different ocular cell types were not affected, they suggest that inhibiting the activity of the VEGFR2 might be an interesting option in the treatment of ocular diseases associated with deregulation of VEGF-A.

Acknowledgements

The authors thank Edith Glass, Nadine Gubernath, Christine Oeruen and Sarah Scislowski for expert technical assistance. They are also grateful to Helmut Deissler, Ulm, Germany for his advice and for supporting the preparation of the manuscript. The authors have no ethical conflicts to disclose. There are no conflicts of interest to declare concerning data generated in this study. This research did not receive any specific grants from funding sources in the public, commercial, or not-for-profit sector.

Appendix A. Supplementary data

Supplementary data to this article can be found online at https://doi.org/10.1016/j.exer.2020.108004.

Author contribution

HLD, MR: design and analyses of experiments, supervision of technicians and research personal performing experiments, analyses of data, writing of manuscript, approval of final version. **J-N S:** performance of experiments, analyses of data, approval of final version. **GEL, GKL, SG:** supervision of research personal, writing of manuscript, approval of final version.

References

Ablonczy, Z., Crosson, C.E., 2007. VEGF modulation of retinal pigment epithelium resistance. Exp. Eye Res. 85, 762–771.

Ablonczy, Z., Prakasam, A., Fant, J., Fauq, A., Crosson, C., Sambamurti, K., 2009. Pigment epithelium-derived factor maintains retinal pigment epithelium function by inhibiting vascular endothelial growth factor-R2 signaling through γ-secretase. J. Biol. Chem. 284, 30177–30186. https://doi.org/10.1074/jbc.M109.032391.

Ablonczy, Z., Dahrouj, M., Tang, P.H., Liu, Y., Sambamurti, K., Marmorstein, A.D., Crosson, C.E., 2011. Human retinal pigment epithelium cells as functional models for the RPE in vivo. Invest. Ophthalmol. Vis. Sci. 52, 8614–8620.

Aiello, L.P., Avery, R.L., Arrigg, P.G., Keyt, B.A., Jampel, H.D., Shah, S.T., Pasquale, L.R., Thieme, H., Iwamoto, M.A., Park, J.E., Nguyen, H.V., Aiello, L.M., Ferrara, N., King, G.L., 1994. Vascular endothelial growth factor in ocular fluid of patients with diabetic retinopathy and other retinal disorders. N. Engl. J. Med. 331, 1480–1487.

Ambati, J., Ambati, B.K., Yoo, S.H., Ianchulev, S., Adamis, A.P., 2003. Age-related macular degeneration: etiology, pathogenesis, and therapeutic strategies. Surv. Ophthalmol. 48, 257–293.

Antonetti, D.A., Barber, A.J., Hollinger, L.A., Wolpert, E.B., Gardner, T.W., 1999. Vascular endothelial growth factor induces rapid phosphorylation of tight junction proteins occludin and zonula occludens 1. J. Biol. Chem. 274, 23463–23467.

Bai, Y., Yu, W., Han, N., Yang, F., Sun, Y., Zhang, L., Zhao, M., Huang, L., Zhou, A., Wang, F., Li, X., 2013. Effects of semaphorin 3A on retinal pigment epithelial cell activity. Invest. Ophthalmol. Vis. Sci. 54, 6628–6638. https://doi.org/10.1167/iovs.13-12625.

Byeon, S.H., Lee, S.C., Choi, S.H., Lee, H.K., Lee, J.H., Chu, Y.K., Kwon, O.W., 2010. Vascular endothelial growth factor as an autocrine survival factor for retinal pigment epithelial cells under oxidative stress via the VEGFR-2/PI3K/Akt pathway. Invest. Ophthalmol. Vis. Sci. 51, 1190–1197. https://doi.org/10.1167/iovs.09-4144.

Campochiaro, P.A., 2000. Retinal and choroidal neovascularization. J. Cell. Physiol. 184, 301–310.

Campochiaro, P.A., 2013. Ocular neovascularization. J. Mol. Med. 91, 311–321.

Castellon, R., Hamdi, H.K., Sacerio, I., Aoki, A.M., Kenney, M.C., Ljubimov, A.V., 2002. Effects of angiogenic growth factor combinations on retinal endothelial cells. Exp. Eye Res. 74, 523–535.

Cunha-Vaz, J., 2017. The blood-retinal barrier in the management of retinal disease: EURETINA award lecture. Ophthalmologica 237, 1–10.

Deissler, H., Deissler, H., Lang, G.K., Lang, G.E., 2005. Generation and characterization of iBREC: novel hTERT-immortalized bovine retinal endothelial cells. Int. J. Mol. Med. 15, 65–70. https://doi.org/10.3892/ijmm.16.1.65.

Deissler, H., Deissler, H., Lang, S., Lang, G.E., 2008. VEGF-induced effects on proliferation, migration and tight junctions are restored by ranibizumab (Lucentis®) in microvascular retinal endothelial cells. Br. J. Ophthalmol. 92, 839–843. https://doi.org/10.1136/bjo.2007.135640.

Deissler, H., Deissler, H., Lang, G.E., 2011. Inhibition of VEGF is sufficient to completely restore barrier malfunction induced by growth factors in microvascular retinal endothelial cells. Br. J. Ophthalmol. 95, 1151–1156. https://doi.org/10.1136/bjo.2010.192229.

Deissler, H.L., Deissler, H., Lang, G.K., Lang, G.E., 2013a. VEGF but not PlGF disturbs the barrier of retinal endothelial cells. Exp. Eye Res. 115, 162–171. https://doi.org/10.1016/j.exer.2013.07.018.

Deissler, H.L., Deissler, H., Lang, G.K., Lang, G.E., 2013b. Ranibizumab efficiently blocks migration but not proliferation induced by growth factor combinations including VEGF in retinal endothelial cells. Graefes Arch. Clin. Exp. Ophthalmol. 251, 2345–2353. https://doi.org/10.1007/s00417-013-2393-5.

Deissler, H.L., Lang, G.K., Lang, G.E., 2015. Binding of VEGF-A is sufficient to abrogate the disturbing effects of VEGF-B together with VEGF-A on retinal endothelial cells. Graefes Arch. Clin. Exp. Ophthalmol. 253, 885–894. https://doi.org/10.1007/s00417-015-2944-z.

Deissler, H.L., Lang, G.K., Lang, G.E., 2017. Inhibition of single routes of intracellular signaling is not sufficient to neutralize the biphasic disturbance of a retinal endothelial cell barrier induced by VEGF-A_{165}. Cell. Physiol. Biochem. 42, 1493–1513. https://doi.org/10.1159/000479213.

Dejana, E., Tournier-Lasserve, E., Weinstein, B.M., 2009. The control of vascular integrity by endothelial cell junctions: molecular basis and pathological implications. Dev. Cell 16, 209–221.

Dunn, K.C., Aotaki-Keen, A.E., Putkey, F.R., Hjelmeland, L.M., 1996. ARPE-19, a human retinal pigment epithelial cell line with differentiated properties. Exp. Eye Res. 62, 155–169. https://doi.org/10.1006/exer.1996.0020.

Dunn, K.C., Marmorstein, A.D., Bonilha, V.L., Rodriguez-Boulan, E., Giordano, F., Hjelmeland, L.M., 1998. Use of the ARPE-19 cell line as a model of RPE polarity: basolateral secretion of FGF5. Invest. Ophthalmol. Vis. Sci. 39, 2744–2749.

Dunn, E.N., Hariprasad, S.M., Sheth, V.S., 2017. An overview of the fovista and rinucumab trials and the fate of anti-PDGF medications. Ophthalmic Surg Lasers Imaging Retina 48, 100–104.

Ferrara, N., 2004. Vascular endothelial growth factor: basic science and clinical progress. Endocr. Rev. 25, 581–611.

Ford, K.M., Saint-Geniez, M., Walshe, T., Zahr, A., D'amore, P.A., 2011. Expression and role of VEGF in the adult retinal pigment epithelium. Invest. Ophthalmol. Vis. Sci. 52, 9478–9487.

Ford, K.M., D'Amore, P.A., 2012. Molecular regulation of vascular endothelial growth factor expression in the retinal pigment epithelium. Mol. Vis. 18, 519–527.

Geisen, P., McColm, J.R., King, B.M., Hartnett, M.E., 2006. Characterization of barrier properties and inducible VEGF expression of several types of retinal pigment epithelium in medium-term culture. Curr. Eye Res. 31, 739–748. https://doi.org/10.1080/02713680600837408.

Hilberg, F., Roth, G.J., Krssak, M., Kautschitsch, S., Sommergruber, W., Tontsch-Grunt, U., Garin-Chesa, P., Bader, G., Zoephel, A., Quant, J., Heckel, A., Rettig, W.J., 2008. BIBF1120: triple angiokinase inhibitor with sustained receptor blockade and good antitumor efficacy. Canc. Res. 68, 4774–4782. https://doi.org/10.1158/0008-5472.CAN-07-6307.

Jeong, J.H., Nguyen, H.K., Lee, J.E., Suh, W., 2016. Therapeutic effect of apatinib-loaded nanoparticles on diabetes-induced retinal vascular leakage. Int. J. Nanomed. 11, 3101–3109.

Kannan, R., Zhang, N., Sreekumar, P.G., Spee, C.K., Rodriguez, A., Barron, E., Hinton, D.R., 2006. Stimulation of apical and basolateral VEGF-A and VEGF-C secretion by oxidative stress in polarized retinal pigment epithelial cells. Mol. Vis. 12, 1649–1659.

Kim, S.R., Suh, W., 2017. Beneficial effects of the Src inhibitor, dasatinib on breakdown of the blood-retinal barrier. Arch Pharm. Res. (Seoul) 40, 197–203. https://doi.org/10.1007/s12272-016-0872-z.

Klettner, A., Möhle, F., Roider, J., 2010. Intracellular Bevacizumab reduces phagocytotic uptake in RPE cells. Graefes Arch. Clin. Exp. Ophthalmol. 248, 819–824. https://doi.org/10.1007/s00417-010-1317-x.

Klettner, A., Westhues, D., Lassen, J., Bartsch, S., Roider, J., 2013. Regulation of constitutive vascular endothelial growth factor secretion in retinal pigment epithelium/choroid organ cultures: p38, nuclear factor κB, and the vascular endothelial growth factor receptor-2/phosphatidylinositol 3 kinase. Mol. Vis. 19, 281–291.

Kliffen, M., Sharma, H.S., Mooy, C.M., Kerkvliet, S., de Jong, P.T., 1997. Increased expression of angiogenic growth factors in age-related maculopathy. Br. J. Ophthalmol. 81, 154–162. https://doi.org/10.1136/bjo.81.2.154.

Kozlowski, M.R., 2015. The ARPE-19 cell line: mortality status and utility in macular degeneration research. Curr. Eye Res. 40, 501–509. https://doi.org/10.3109/02713683.2014.935440.

Li, D., Xie, K., Zhang, L., Yao, X., Li, H., Xu, Q., Wang, X., Jiang, J., Fang, J., 2016. Dual blockade of vascular endothelial growth factor (VEGF) and basic fibroblast growth factor (FGF-2) exhibits potent anti-angiogenic effects. Canc. Lett. 377, 164–173. https://doi.org/10.1016/j.canlet.2016.04.036.

McLaren, M.J., Inana, G., 1997. Inherited retinal degeneration: basic FGF induces phagocytic competence in cultured RPE cells from RCS rats. FEBS Letters 412, 21–29. https://doi.org/10.1016/s0014-5793(97)00566-8.

Miki, A., Miki, K., Ueno, S., Wersinger, D.M., Berlinicke, C., Shaw, G.C., Usui, S., Wang, Y., Zack, D.J., Campochiaro, P.A., 2010. Prolonged blockade of VEGF receptors does not damage retinal photoreceptors or ganglion cells. J. Cell. Physiol. 224, 262–272. https://doi.org/10.1002/jcp.22129.

Miura, Y., Klettner, A., Roider, J., 2010. VEGF antagonists decrease barrier function of retinal pigment epithelium in vitro: possible participation of intracellular glutathione. Invest. Ophthalmol. Vis. Sci. 51, 4848–4855. https://doi.org/10.1167/iovs.09-4699.

Miyamoto, N., de Kozak, Y., Jeanny, J.C., Glotin, A., Mascarelli, F., Massin, P., BenEzra, D., Behar-Cohen, F., 2007. Placental growth factor-1 and epithelial haemato-retinal barrier breakdown: potential implication in the pathogenesis of diabetic retinopathy. Diabetologia 50, 461–470.

Nagineni, C., Kutty, V., Detrick, B., Hooks, J.J., 2005. Expression of PDGF and their receptors in human retinal pigment epithelial cells and fibroblasts: regulation by TGF-beta. J. Cell. Physiol. 203, 35–43.

Nakamura, K., Taguchi, E., Miura, T., Yamamoto, A., Takahashi, K., Bichat, F., Guilbaud, N., Hasegawa, K., Kubo, K., Fujiwara, Y., Suzuki, R., Kubo, K., Shibuya, M., Isae, T., 2006. KRN951, a highly potent inhibitor of vascular endothelial growth factor receptor tyrosine kinases, has antitumor activities and affects functional vascular properties. Canc. Res. 66, 9134–9142.

Oh, H., Takagi, H., Otani, A., Koyama, S., Kemmochi, S., Uemura, A., Honda, Y., 2002. Selective induction of neuropilin-1 by vascular endothelial growth factor(VEGF): a mechanism contributing to VEGF-induced angiogenesis. Proc. Natl. Acad. Sci. U.S.A. 99, 383–388.

Ozaki, H., Yu, A.Y., Della, N., Ozaki, K., Luna, D.J., Yamada, H., Hackett, S.F., Okamoto, N., Zack, D.F., Semenzy, G.L., Campochiaro, P.A., 1999. Hypoxia inducible factor-1alpha is increased in ischemic retina: temporal and spatial correlation with VEGF expression. Invest. Ophthalmol. Vis. Sci. 40, 182–189.

Pan, Q., Chathery, Y., Wu, Y., Rathore, N., Tong, R.K., Peale, F., Bagri, A., Tessier-Lavigne, M., Koch, A.W., Watts, R.J., 2007. Neuropilin-1 binds to VEGF121 and regulates endothelial cell migration and sprouting. J. Biol. Chem. 282, 24049–24056.

Qaum, T., Xu, Q., Joussen, A.M., Clemens, M.W., Qin, W., Miyamoto, K., Hassessian, H., Wiegand, S.J., Rudge, J., Yancopoulos, G.D., Adamis, A.P., 2001. VEGF-initiated blood-retinal barrier breakdown in early diabetes. Invest. Ophthalmol. Vis. Sci. 42, 2408–2413.

Ranjbar, M., Brinkmann, M.P., Zapf, D., Miura, Y., Rudolf, M., Grisanti, S., 2016a. Fc receptor inhibition reduces susceptibility to oxidative stress in human RPE cells treated with bevacizumab, but not aflibercept. Cell. Physiol. Biochem. 38, 737–747. https://doi.org/10.1159/000443030.

Ranjbar, M., Brinkmann, M.P., Tura, A., Rudolf, M., Miura, Y., Grisanti, S., 2016b. Ranibizumab interacts with the VEGF-A/VEGFR-2 signaling pathway in human RPE cells at different levels. Cytokine 83, 210–216. https://doi.org/10.1016/j.cyto.2016.04.014.

Saint-Geniez, M., Maharaj, A.S., Walshe, T.E., Tucker, B.A., Sekiyama, E., Kurihara, T., Darland, D.C., Young, M.J., D'Amore, P.A., 2008. Endogenous VEGF is required for visual function: evidence for a survival role on Müller cells and photoreceptors. PloS One 3, e3554. https://doi.org/10.1371/journal.pone.0003554.

Schottler, J., Randoll, N., Lucius, R., Caliebe, A., Roider, J., Klettner, A., 2018. Long-term treatment with anti-VEGF does not induce cell aging in primary retinal pigment epithelium. Exp. Eye Res. 171, 1–11. https://doi.org/10.1016/j.exer.2018.03.002.

Stahl, A., Paschek, L., Martin, G., Feltgen, N., Hansen, L.L., Agostini, H.T., 2009. Combinatory inhibition of VEGF and FGF2 is superior to solitary VEGF inhibition in an in vitro model of RPE-induced angiogenesis. Graefes Arch. Clin. Exp. Ophthalmol. 247, 767–773. https://doi.org/10.1007/s00417-009-1058-x.

Starzec, A., Vassy, R., Martin, A., Lecouvey, M., Di Benedetto, M., Crépin, M., Perret, G.Y., 2006. Antiangiogenic and antitumor activities of peptide inhibiting the vascular endothelial growth factor binding to neuropilin-1. Life Sci. 79, 2370–2381.

Strauss, O., 2005. The retinal pigment epithelium in visual function. Physiol. Rev. 85, 845–881.

Suarez, S., McCollum, G.W., Bretz, C.A., Yang, R., Capozzi, M.E., Penn, J.S., 2014. Modulation of VEGF-induced retinal vascular permeability by peroxisome proliferator-activated receptor-β/δ. Invest. Ophthalmol. Vis. Sci. 55, 8232–8240. https://doi.org/10.1167/iovs.14-14217.

Sun, M., Fu, H., Cheng, H., Cao, Q., Zhao, Y., Mou, X., Zhang, X., Liu, X., Ke, Y., 2012. A dynamic real-time method for monitoring epithelial barrier function in vitro. Anal. Biochem. 425, 96–103. https://doi.org/10.1016/j.ab.2012.03.010.

Tirand, L., Frochot, C., Vanderesse, R., Thomas, N., Trinquet, E., Pinel, S., Viriot, M.L., Guillemin, F., Barberi-Heyob, M., 2006. A peptide competing with VEGF165 binding on neuropilin-1 mediates targeting of a chlorin-type photosensitizer and potentiates its photodynamic activity in human endothelial cells. J. Contr. Release 111, 153–164.

Whittles, C.E., Pocock, T.M., Wedge, S.R., Kendrew, J., Hennequin, L.F., Harper, S.J., Bates, D.O., 2002. ZM323881, a novel inhibitor of vascular endothelial growth factor-receptor 2 tyrosine kinase activity. Microcirculation 9, 513–522.

Zhou, L., Sun, X., Huang, Z., Zhou, T., Zhu, X., Liu, Y., Wang, J., Cheng, B., Li, M., He, C., Liu, X., 2018. Imatinib ameliorated retinal neovascularization by suppressing PDGFR-α and PDGFR-β. Cell. Physiol. Biochem. 48, 263–273. https://doi.org/10.1159/000491726.